BIODIVERSITAS
Volume 24, Number 3, March 2023
Pages: 1742-1748

ISSN: 1412-033X
E-ISSN: 2085-4722
DOI: 10.13057/biodiv/d240348

Characterization of silver nanoparticles (AgNPs) synthesized from *Piper ornatum* leaf extract and its activity against food borne pathogen *Staphylococcus aureus*

FIRLI RAHMAH PRIMULA DEWI[1,♥], VUANGHAO LIM[2], A'LIYATUR ROSYIDAH[3], FATIMAH[1], SRI PUJI ASTUTI WAHYUNINGSIH[1], UMMI ZUBAIDAH[1]

[1]Department of Biology, Faculty of Science and Technology, Universitas Airlangga. Jl. Dr. Ir. Soekarno, Surabaya 60115, East Java, Indonesia. Tel./fax.: +62-311-5936501, ♥email: firli.rahmah@fst.unair.ac.id
[2]Advanced Medical and Dental Institute, Universiti Sains Malaysia. Bertam 13200 Kepala Batas, Penang, Malaysia
[3]Research Center for Vaccine and Drug, National Research and Innovation Agency. Jl. Raya Jakarta-Bogor Km 46, Bogor 16911, West Java, Indonesia

Manuscript received: 20 January 2023. Revision accepted: 23 March 2023.

Abstract. *Dewi FRP, Lim V, Rosyidah A, Fatimah, Wahyuningsih SPA, Zubaidah U. 2023. Characterization of silver nanoparticles (AgNPs) synthesized from* Piper ornatum *leaf extract and its activity against food borne pathogen* Staphylococcus aureus*. Biodiversitas 24: 1742-1748. Staphylococcus aureus* is the most recurrent food borne pathogen that commonly resists antibiotics. Silver nanoparticles (AgNPs) have potential to solve bacterial multidrug resistance. This study aims to assess bactericidal activity of AgNPs against *S. aureus* synthesized from *Piper ornatum* leaf extract. Biosynthesis was performed by mixing *P. ornatum* extract with $AgNO_3$ aqueous solution and then incubating for 24 h at room temperature under dark condition. The formation of AgNPs was confirmed by changing optical color from light yellowish to dark brown with a peak of UV spectrum at ~500 nm. According to SEM imaging, AgNPs had spherical form whereas EDS analysis revealed strong signal at 3 kV indicating existence of silver element. Meanwhile, face-centered cubic structures of AgNPs were indicated by XRD analysis. FTIR analysis confirmed ketone, flouro, and amine as functional groups presented in extract were essential for the bioreduction of silver nitrate to silver nanoparticles. This study revealed that AgNPs have a potent bactericidal effect. In vitro evaluation using agar well-diffusion assay showed high inhibition zone of *S. aureus* (14.28±0.26) upon treating with 25 µg/mL AgNPs while MIC value was 5 µg/mL. However, antibiotic erythromycin and chloramphenicol respectively exhibited better inhibition zone and MIC value.

Keywords: AgNPs, bactericidal activity, human and health, in vitro assay, *Piper ornatum, Staphylococcus aureus*

INTRODUCTION

The recent global burden of bacterial infection is the ability of bacteria to tolerate antimicrobial agents. Many species of bacteria were advanced enough to resist antimicrobial agents long before humans began to mass-produce them in order to address either preventing or treating bacterial infections (Larsson and Flach 2022). Globally, about 4.95 million (3.62-6.57) deaths associated-antimicrobial resistance were reported in 2019. In addition, estimation of all-age death rate associated with antimicrobial resistance is highest in western sub-Saharan Africa with 27.3 deaths per 100,000 (20.9-35.3) and lowest in Australasia with 6.5 deaths (4.3-9.4) per 100,000. The six bacterial species that majority lead to deaths associated with resistance were *Escherichia coli*, *Staphylococcus aureus, Klebsiella pneumoniae, Streptococcus pneumoniae*, *Acinetobacter baumannii*, and *Pseudomonas aeruginosa*. They are responsible for causing 929,000 (660,000-1,270,000) mortalities attributable to antimicrobial resistance and also caused 3.57 million (2.62-4.78) deaths associated with antimicrobial resistance in 2019 (Murray et al. 2022).

Staphylococcus aureus is a Gram-negative bacteria which among the most frequently food borne pathogen causing morbidity and mortality. This pathogen leads to wide variety of ailments, ranging from moderately severe skin infections to fatal pneumonia and sepsis. *S. aureus* infection is getting more complicated due to frequently occurring antibiotic resistance in which methicillin-resistant *S. aureus* (MRSA) has been well-known for antimicrobial resistance case (Cheung et al. 2021). MRSA was reported to give rise to more than 100,000 deaths associated with antimicrobial resistance in 2019 (Murray et al. 2022). Hence, novel and effective antimicrobial agent against antibiotic-resistant bacteria is very urgently generated. In this respect, nanoparticles are vividly acknowledged for their potency as antimicrobial agents. Even more, nanoparticles are considered to become viable alternative to antibiotic in solving bacterial multidrug resistance problems (Franci et al. 2015). Nanoparticles can enter cell wall and membrane of bacteria which further disturb important molecular mechanisms, leading to bacterial collapse (Ozdal and Gurkok 2022). Among other nanoparticles originating from noble metals, silver nanoparticles (AgNPs) have gained much interest as antimicrobial in the scientific field. This is because silver is broadly used as an antiseptic and antimicrobial against Gram-positive and Gram-negative bacteria (Franci et al. 2015).

A variety of preparation methods have been elucidated for the synthesis of AgNPs, ranging from physical, chemical, and biological synthesis (Iravani et al. 2014). The use of physiochemical methods are in fact durable and technically viable, but large-scale production is highly restricted since it creates high cost, energy, and time-consuming while waste purification is burdensome. Here, green synthesis of AgNPs that used several microorganisms, plants, and algae is considerable due to biocompatible and environmentally safe. Among other biomaterials, plant is considerably and more beneficial for AgNPs synthesis (Masum et al. 2019). Besides abundant sources, plant materials offer no threat of contamination compared to bacterial and chemical materials while less energy utilization and easiness are also demandable (Masum et al. 2019). Bioactive compounds of plant such as polyphenols, flavonoids, terpenoids, tannins, alkaloids, amines, ketones, and aldehydes can mediate conversion of silver ions to silver nanoparticles by acting as reducing, stabilizing, and capping agent (Hemlata et al. 2020).

In the term of folklore medicine, *Piper* genus is found to be abundantly used as analgesic, antibacterial, and antioxidant agent among people in South and Southeast Asia. Interestingly, this plant host secondary metabolites with polyphenolic, conjugated, and hemiacetal structures which has the potential to reduce Ag^+ to Ag^0 (Mahiuddin et al. 2020). Recent research revealed successful biosynthesis of AgNPs using various species of Piperaceae family, including *Piper chaba* (Mahiuddin et al. 2020), *Piper colubrinum* (Santhoshkumar et al. 2021), *Piper nigrum* (Paulkumar et al. 2014), *Piper betle* (Lagashetty et al. 2019), and *Piper longum* (Jamila et al. 2020) This product of AgNPs is evaluated for antibacterial effect against *Bacillus cereus*, *Escherichia coli*, *Klebsiella pneumonia*, *Staphylococcus aureus* and it conveyed high level of inhibition (Santhoshkumar et al. 2021). However, the use of *Piper ornatum* to synthesize AgNPs is not reported yet. This study aimed to highlight the potency of *P. ornatum* extract to mediate reduction of silver ion into silver nanoparticle. The nano-silver product was further assessed for antimicrobial activity comprising *in vitro* antibacterial activity and minimum inhibitory concentration (MIC) against *S. aureus* infection.

MATERIALS AND METHODS

Subject to AgNPs biosynthesis, silver nitrate (MERCK) and fresh leaves of *P. ornatum* (obtained from Surabaya, Indonesia) were prepared. *S. aureus* (ATCC 25923 PK/5) were cultured in Mueller-Hinton broth (MHB) medium and incubated in shaker incubator (37ºC; 150 rpm) and conditioned to reach 0.1 in OD_{600} prior to use. Preparation of *P. ornatum* extract and biosynthesis of AgNPs. Extraction of *P. ornatum* followed procedure reported by Masum et al. (2019) with no modification. Fresh leaves of *P. ornatum* (Figure 1.A) were washed with deionized water (dH_2O). Subsequently, as much as 20 g of fresh leaf was finely macerated together with 100 mL sterile dH_2O using a blender to get 10% (w/v) broth extract. Afterward, the extract was purified with a muslin cloth and Whatman No. 1 filters paper respectively which then kept at 4ºC until further use. In order to biosynthesize AgNPs, about 20 mL broth extract was mixed with 180 mL aqueous solution of $AgNO_3$ (0.1 M) and then incubated at room temperature under dark condition for 24 h. The reduction of silver ion was confirmed by changing optical color into dark brown and measured using spectrophotometer UV-vis at 200-800 nm with interval 2 nm of wavelength.

Characterization of AgNPs

The FTIR spectroscopy measurement of *P. ornatum* extract and AgNPs was performed using FTIR (Perkin Elmer FTIR Spectrometer Spectrum Two) in the 4000-400 cm^{-1} range. The extract and AgNPs powder were placed in the diamond chamber, and the spectra were immediately recorded. A signal from an empty chamber was subtracted for each sample as a background. The spectral data were compared to the database to determine the functional group in each sample (Weeranantanapan et al. 2022). The FT-IR analysis was conducted at the Integrated Laboratory of Bioproduct (iLab), National Research and Innovation Agency (BRIN), Indonesia.

X-ray diffraction (XRD) was used to examine the crystallinity of biologically produced AgNPs (D Advance, Bruker, Germany). The AgNPs were prepared by freeze-drying, and a diffraction pattern was scanned in the range of 2θ from 20° to 80° (Weeranantanapan et al. 2022). The XRD analysis was conducted at the Integrated Laboratory of Bioproduct (iLab), National Research and Innovation Agency (BRIN), Indonesia.

The morphology of synthesized AgNPs was studied using a scanning electron microscope (Quattro S SEM, Thermo Scientific). EDS (OXFORD Instrument) was used to confirm the sample's elemental silver and other chemical compositions (Rosyidah et al. 2021). The SEM and EDS analysis was conducted at the Integrated Laboratory of Bioproduct (iLab), National Research and Innovation Agency (BRIN), Indonesia.

Inoculum preparation of *S. aureus*

Staphylococcus aureus ATCC 25923 was obtained from the Microbiology Laboratory, Department of Biology, Universitas Airlangga, Indonesia. Overnight culture was prepared by transferring a colony of *S. aureus* ATCC 25923 in Muller-Hinton Broth (MHB) then was incubated overnight at 37°C (150 rpm).

In vitro evaluation of AgNPs antimicrobial effect

Agar well-diffusion technique was carried out to know inhibition effect of extract against *S. aureus*. Into petri dish containing Muller Hinton Agar (MHA) media, suspension of *S. aureus* (OD_{600} = 0.1; 100 µL) was added then spread using sterile cotton swab. Various concentrations of AgNPs (5, 12.5, 25, and 50 µg/mL) with 30 µL volume of each was placed into well within media. Here, erythromycin was used as positive control. Incubation was done for 24 h at 30ºC. Hollow zone formed around well was denoted as inhibitory activity of AgNPs against *S. aureus*.

Determination of Minimum Inhibitory Concentration (MIC)

Series concentrations (5, 10, 20, and 30 µg/mL) of AgNps solution were added to MHB media containing 104 CFU/mL in a 96-well microplate. Chloramphenicol was used as positive control. The OD at 600 nm was read before and after 24 h incubation at 37ºC using a microplate reader. The minimum inhibitory concentration (MIC) was defined as the lowest concentration of AgNPs solution that inhibit *S. aureus*'s growth as indicated by no increase of OD_{600} value upon 24 h incubation.

RESULTS AND DISCUSSION

Synthesis and characterization of AgNPs

A rapid reduction of Ag^+ to Ag^0 in $AgNO_3$ solution after mixed with *P. ornatum* extract was indicated by color change from light yellowish to dark brown (Figure 1B). UV-vis spectroscopy is used to further confirm the formation and stability of AgNPs in aqueous solution (Bhuvaneswari et al. 2014). There was an alteration of absorbance in the UV spectrum where peak of AgNPs was confirmed in the wavelength of ~500 nm (Figure 1C). FTIR analysis was used to identify the phytochemical compound that acts as reducing, capping, and stabilizing agent of AgNPs. The assignments of *P. ornatum* were observed in Figure 2A. The band at 3285 cm^{-1} corresponded to the N-H stretching of primary amine. The peak at 2918 cm^{-1} was associated with the C-H stretching of alkanes. The peak at 1621 cm^{-1} indicated the C=O stretching mode of ketones. The peak at 1318 and 1151 cm^{-1} were attributed to the C-N stretching of amine. The 1077 cm^{-1} peak corresponded to ether's C-O stretching and aliphatic fluoro's C-F stretching. The peaks at 575 and 518 cm^{-1} corresponded to the aliphatic iodo compounds, C-I stretching, alcohol, and OH out-of-plane bending. FTIR spectrum of synthesized AgNPs from *P. ornatum* is shown in Figure 2A. The reduction process of AgNPs showed the band at 3286 cm^{-1} which corresponded to N-H stretching of primary amine. An intense peak at 1622 cm^{-1} was attributed to the C=O stretching mode of the ketone. The peak at 1151 and 1077 cm^{-1} corresponded to the amine C-N stretching. Here, we demonstrated that ketone, fluoro, and amine groups regulated transmittance percentages were crucial for the bioreduction of silver nitrate to silver nanoparticles. Similar results were also shown by the synthesis of AgNPs using *P. nigrum* (Krishnan et al. 2016).

The crystalline structure of synthesized AgNPs was confirmed by XRD (Figure 2B). The AgNPs expressed intense peaks at 38.2°, 44.3°, 64.6°, and 76.02°, which corresponded to (111), (200), (220), and (311) planes, respectively. Bragg's peaks at (111), (200), (220), and (311) revealed the formation of face-centered cubic structures of AgNPs. In order to validate the existence of metallic AgNPs in the mixture, further elemental analysis was done. The EDS analysis of AgNPs produced by *P. ornatum* was shown in Figure 2C. The results of the EDS investigation revealed a strong signal at 3 kV that points to the existence of elemental silver. Other elements found in the colloidal sample of AgNPs, such as carbon, oxygen, and chlorine, could be a result of a phytochemical compound signal in the *P. ornatum* extract. The SEM study was used to obtain information on morphology and size of the synthesized AgNPs (Bhuvaneswari et al. 2014). The SEM image of synthesized AgNPs from *P. ornatum* showed a dominantly spherical form (which should be confirmed again using TEM), as shown in Figure 2D.

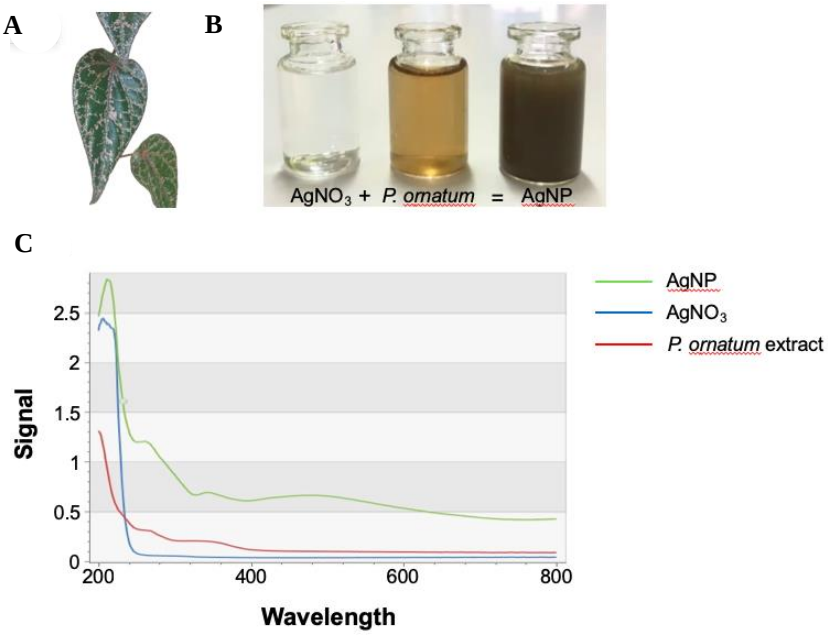

Figure 1. Biosynthesis of silver nanoparticles (AgNPs). A. *P. ornatum* leaf. B. Color changes shown in the *P. ornatum* leaf extract upon addition of 0.1 M silver nitrate ($AgNO_3$) aqueous solution. C. UV-visible spectrum of AgNPs where the peak at ~500 nm indicates the surface plasmon resonance of AgNPs

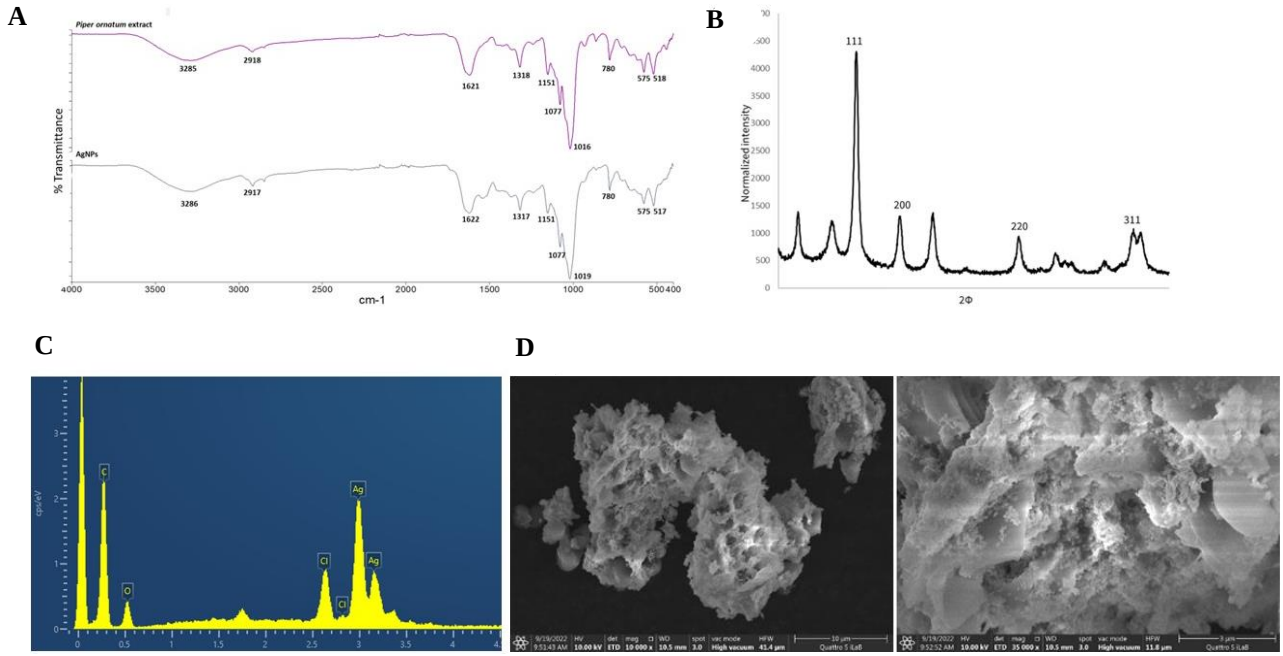

Figure 2. Characterization of AgNPs. A. Fourier transform infrared spectroscopy spectra of *P. ornatum* extract and AgNPs. B. X-Ray diffraction pattern of synthesized AgNPs. C. Elemental composition of synthesized AgNPs. D. SEM imaging that shows morphology of AgNPs under 10,000x (left) and 35,000x (right) magnification

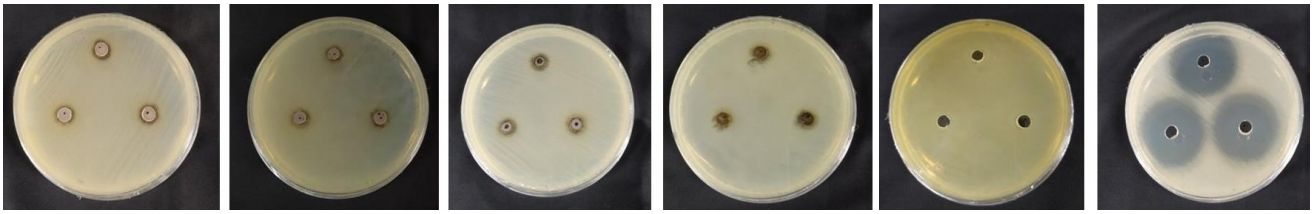

5 µg/mL **12.5 µg/mL** **25 µg/mL** **50 µg/mL** ***S. aureus*** **Erythromycin**

Figure 3. Series concentrations of AgNPs showed different inhibition zone against *S. aureus*. Antibiotic erythromycin is used as positive control

Table 1. The antimicrobial effect of AgNPs mediated by *P. ornatum* leaf extract against *S. aureus*

Concentration of AgNPs (µg/mL)	Inhibition zone (mm)
5	13.52±0.13
12.5	11.93±0.24
25	14.28±0.26
50	13.27±0.82
Erythromycin	48.27±0.46

Table 2. Determination of minimum inhibition concentration of silver nanoparticles (AgNPs) synthesized by *P. ornatum* leaf extract against *S. aureus*

Concentration of AgNPs (µg/mL)	OD_{600}	
	Pre	Post
5	3.04±0.275	0.74±0.048
10	3.78±0.103	0.32±0.124
20	3.77±0.073	0.03±0.06
30	3.85±0.022	0.08±0.07
Chloramphenicol	0.06±0.006	0.03±0.003
S. aureus (negative control)	0.079±0.03	0.34±0.047

Antimicrobial effect of AgNPs against *S. aureus*

Agar well-diffusion assay confirmed inhibition effect of AgNPs towards *S. aureus* growth (Figure 3 and Table 1). Among series concentrations of AgNPs, concentration of 25 µg/mL showed the best inhibition with high inhibition zone (14.28±0.26) but was not far different compared to the lowest concentration 5 µg/mL with inhibition zone 13.52±0.13 mm. Here, antibiotic erythromycin exhibited the highest inhibition effect with inhibition zone 48.27±0.46 mm above all AgNPs concentration.

Minimum Inhibitory Concentration (MIC) value of AgNPs

AgNPs showed potent antimicrobial activity in suppressing the growth of *S. aureus* (Table 2). The reduction of OD_{600} value was followed in dose-dependent manner. Herein, concentration 5 µg/mL was considered as MIC value since it became the lowest concentration that exhibited no increment of OD_{600} value after 24 h of incubation. Even so, chloramphenicol had a post OD value that was better than all concentrations of AgNPs, except concentration 20 µg/mL.

Discussion

Staphylococcus aureus is a food-borne pathogen that is commonly associated with antimicrobial resistance. The prevalence of methicillin-resistant *S. aureus* (MRSA) ranged between 13%-74% around the world (Köck et al. 2010). Methicillin-resistant *S. aureus* with mortality rate 15.6% is significantly higher than methicillin-susceptible *S. aureus* with mortality rate 6.2% (Kang et al. 2010; Hassoun et al. 2017). The problem of MRSA has caused a vivid challenge to recent public health. Research on novel-effective anti- *S. aureus* becomes a noticeable effort. Nanoparticle is known to alternatively replace the use of antibiotic and seem to have high potential in solving bacterial multidrug resistance (Franci et al. 2015). AgNPs, in particular, have a widely described antibacterial effect due to the fact that silver has been used in the past as an antiseptic and antimicrobial against Gram-positive and Gram-negative bacteria (Masum et al. 2019).

Nowadays, the synthesis of AgNPs can be executed by employing either physical, chemical, and biological method (Iravani et al. 2014). Biological synthesis, also known as green synthesis, of nanoparticles that employ plant extract offers advantages due to being biocompatible and environmentally safe. The successful AgNPs synthesis is indicated by ability of plant metabolite compounds to reduce Ag^+ into Ag^0. Several species of *Piper* have been confirmed to have abundant polyphenolic compounds with antioxidant activity which potent to perform Ag^+ reduction (Insanu et al. 2017; Mahiuddin et al. 2020). *P. ornatum* extract could reduce Ag^+ into Ag^0 which was indicated by rapid color change from light yellowish to dark brown (Figure 1B). The synthesized AgNPs were also confirmed by UV spectral analysis where absorption peak centered at ~500 nm indicating the presence of AgNPs (Figure 1C). Free electrons owned by metal nanoparticles, AgNPs in particular, resonance with light wave resulting in a surface plasmon resonance (Bhuvaneswari et al. 2014). Changes in color arise since any excitation of surface plasmon resonance for the synthesized AgNPs (Bhuvaneswari et al. 2014). Gomaa (2017) reported an absorption peak of AgNPs at 420 nm while Bhuvaneswari indicated an absorption peak of AgNPs at 390 nm. The number of synthesized AgNPs is in line with increase in reaction time indicated by increasing intensity of UV absorbance (Bhuvaneswari et al. 2014).

As previously mentioned, bio-reduction of silver ions into AgNPs is mediated by bioactive compounds within plant extract (Hemlata et al. 2020). The FTIR indicated functional groups such as ketone, flouro, and amine that are present in *P. ornatum* extract are responsible for reducing, capping, and stabilizing agents of AgNPs. The same result was also indicated in the synthesis of AgNPs mediated by *P. nigrum* (Krishnan et al. 2016). Moreover, the formation of hydrogen bonds between amine group of *P. chaba* stem extract and the surface of AgNPs was also reported by Mahiuddin et al. (2020), indicating amine group is responsible for capping agent. The recent study reports AgNPs have dominantly spherical form confirmed by SEM analysis. Besides, single surface plasmon resonance is also indicated in recent study that corresponds to spherical nanoparticles (Bhuvaneswari et al. 2014). This result was also supported by Mahiuddin et al. (2020) that revealed homogenous spherical form AgNPs from *P. chaba* with size of 26 nm and almost spherical with homogeneous morphology and Krishnan et al. (2016) that reported spherical form of AgNPs from *P. nigrum* with an average particle size of 20-40 nm. Antibacterial activity of AgNPs strongly depended on the size where smaller dimensions less than 30 nm optimally inhibited *S. aureus* (Collins et al. 2010). Another study by Bhuvaneswari et al. (2014) reported AgNPs synthesized from *Naringi crenulata* extract had cubic beside spherical form within the range of 72-98 nm. Here, the presence of various bioactive molecules within extract can cause optical and electronic properties alteration in the shape of metal nanoparticles (Bhuvaneswari et al. 2014). Further elemental (EDX) analysis confirmed strong signal at 3kV that validates existence of AgNPs in this study. This result is supported by several studies. Bhuvaneswari et al (2014) reported strong signal in the range of 2.5-4 keV indicating metallic nanocrystal synthesized by *Naringi crenulata* extract as well as Vijayakumar et al. (2013) obtained signal in the range of 2-4 keV of square shape AgNPs from *Artemisia nilagirica* leaf extracts. Moreover, Jagtap and Bapat (2013) reported signal at 2.983 keV of irregular shape AgNPs from *Artocarpus heterophyllus* seed extract. The EDX analysis along with SEM imaging provides information on the biochemical analysis of the investigated fields (Bhuvaneswari et al. 2014).

Nowadays, recent antibiotics specific to staphylococci target the cell envelope, ribosome, and nucleic acid (Foster 2017). Recent study reported that AgNPs showed potent antimicrobial against *S. aureus*. According to Theos et al. (2019), the most effective antibiotics against all *S. aureus* cultures were linezolid (100%), trimethoprim sulfamethoxazole (95%) and tetracyclines (94%). Meanwhile, MRSA isolates can be effectively addressed by linezolid (100%) and trimethoprim sulfamethoxazole (100%). However, resistance to several antibiotics such as tetracyclines has already been reported making new alternative antibiotics urgently need to be researched and produced (Foster 2017). Concentration of 25 µg/mL caused high inhibition zone although the result was not far different from concentration of 5 µg/mL in agar-well diffusion assay (Table 1). Meanwhile, concentration of 5 µg/mL was considered as MIC value (Table 2). This finding of MIC value as same as vancomycin-intermediate *Staphylococcus aureus* (VISA) that has an MIC of 4-8 µg/mL (Foster 2017). The correlation between AgNPs concentration and antibacterial effect depends on type of bacteria (Chernousova and Epple 2013). Herein, AgNPs definitely exhibit an effective bactericidal effect against *E. coli* and *S. aureus* (Jain et al. 2009). This support result of recent study that the lowest concentration (5 µg/mL) could show good inhibition. In the case of Gram-negative bacteria, AgNPs attach and accumulate into bacterial surface making cell membrane more permeable which further cause irreversible cell damage (Lazar et al. 2021). This action mechanism is strongly affected by the size, shape, and concentration of nanoparticles. Accumulation of

AgNPs on the bacterial membrane cell makes gap in the phospholipid bilayer which further predispose it to a permeability increment and ends with bacterial cell death. The smaller size of AgNPs (<30 nm) and positive zeta potential were optimal against *S. aureus*. This is because electrostatic forces of AgNPs with positive zeta potential face negative surface charge of bacteria leading to a closer interaction between the two entities and possibly ending with bacterial membranes penetration (Franci et al. 2015). Moreover, AgNPs can induce release of reactive oxygen species (ROS) that is known for powerful antibacterial action. Mechanisms of bacterial destruction owned by AgNPs seem to work in synergy comprising cell wall disruption, free radical formation and intercalation between DNA bases (Franci et al. 2015).

In conclusion, biosynthesis of AgNPs using *P. ornatum* leaves extract has been successfully performed. Rapid color change indicates the reduction of Ag^+ into Ag^0. AgNPs have a spherical form shown by SEM and their existence is validated by EDS. Ketone, fluoro, and amine groups found in extract are responsible for reducing, capping, and stabilizing agents of AgNPs. AgNPs exhibited bactericidal effect against *S. aureus* with the best inhibition zone at 25 µg/mL while MIC value was 5 µg/mL.

ACKNOWLEDGEMENTS

The materials and publication fee for this study were financially supported by SATU-JRS research funding 2022 (grant number: 1272/UN3.15/PT/2022).

REFERENCES

Bhuvaneswari T, Thiyagarajan M, Geetha N, Venkatachalam P. 2014. Bioactive compound loaded stable silver nanoparticle synthesis from microwave irradiated aqueous extracellular leaf extracts of *Naringi crenulata* and its wound healing activity in experimental rat model. Acta Tropica 13:, 55-61. DOI: 10.1016/j.actatropica.2014.03.009.

Chernousova S, Epple M. 2013. Silver as antibacterial agent: Ion, nanoparticle, and metal. Angew Chem Int Ed Engl 52: 1636-1653. DOI: 10.1002/anie.201205923.

Cheung GY, Bae JS, Otto M. 2021. Pathogenicity and virulence of *Staphylococcus aureus*. Virulence 12: 547-569. DOI: 10.1080/21505594.2021.1878688.

Collins TL, Markus EA, Hassett DJ, Robinson JB. 2010. The effect of a cationic porphyrin on *Pseudomonas aeruginosa* biofilms. Curr Microbiol 61: 411-416. DOI: 10.1007/s00284-010-9629-y.

Foster TJ. 2017. Antibiotic resistance in *Staphylococcus aureus*: Current status and future prospects. FEMS Microbiol Rev 41 (3): 430-449. DOI: 10.1093/femsre/fux007.

Franci G, Falanga A, Galdiero S, Palomba L, Rai M, Morelli G, Galdiero M. 2015. Silver nanoparticles as potential antibacterial agents. Molecules 20: 8856-8874. DOI: 10.3390/molecules20058856.

Gomaa EZ. 2017. Silver nanoparticles as an antimicrobial agent: A case study on *Staphylococcus aureus* and *Escherichia coli* as models for Gram-positive and Gram-negative bacteria. J Gen Appl Microbiol 63 (1): 36-43. DOI: 10.2323/jgam.2016.07.004.

Hassoun A, Linden PK, Friedman B. 2017. Incidence, prevalence, and management of MRSA bacteremia across patient populations: A review of recent developments in MRSA management and treatment. Critical Care 21: 1-10. DOI: DOI: 10.1186/s13054-017-1801-3.

Hemlata, Meena PR, Singh AP, Tejavath KK. 2020. Biosynthesis of silver nanoparticles using *Cucumis prophetarum* aqueous leaf extract and their antibacterial and antiproliferative activity against cancer cell lines. ACS Omega 5: 5520-5528. DOI: 10.1021/acsomega.0c00155.

Insanu M, Marliani L, Dinilah NP. 2017. Comparison of antioxidant activities from four species of piper. Pharmaciana 7: 305. DOI: 10.12928/pharmaciana.v7i2.6935.

Iravani S, Korbekandi H, Mirmohammadi SV, Zolfaghari B. 2014. Synthesis of silver nanoparticles: Chemical, physical and biological methods. Res Pharm Sci 9 (6): 385-406.

Jagtap UB, Bapat VA. 2013. Green synthesis of silver nanoparticles using *Artocarpus heterophyllus* Lam. seed extract and its antibacterial activity. Ind Crops Prod 46: 132-132. DOI: 10.1016/j.indcrop.2013.01.019.

Jain D, Daima HK, Kachhwaha S, Kothari SL. 2009. Synthesis of plant-mediated silver nanoparticles using papaya fruit extract and evaluation of their antimicrobial activities. Digest J Nanomaterials Biostructures 4 (3): 557-563.

Jamila N, Khan N, Bibi A, Haider A, Khan SN, Atlas A et al. 2020. *Piper longum* catkin extract mediated synthesis of Ag, Cu, and Ni nanoparticles and their applications as biological and environmental remediation agents. Arab J Chem 13: 6425-6436. DOI: 10.1016/j.arabjc.2020.06.001.

Kang CI, Song JH, Chung DR., Peck KR, Ko KS, Yeom, JS, Asian Network for Surveillance of Resistant Pathogens (ANSORP) Study Group. 2010. Clinical impact of methicillin resistance on outcome of patients with *Staphylococcus aureus* infection: A stratified analysis according to underlying diseases and sites of infection in a large prospective cohort. J Infect 61 (4): 299-306.

Köck R, Becker K, Cookson B, van Gemert-Pijnen JE, Harbarth S, Kluytmans J, Mielke M, Peters G, Skov RL, Struelens MJ, Tacconelli E, Torné AN, Witte W, Friedrich AW. 2010. Methicillin-resistant *Staphylococcus aureus* (MRSA): Burden of disease and control challenges in Europe. Euro Surveill 15 (41): 19688. DOI: 10.2807/ese.15.41.19688-en.

Krishnan V, Bupesh G, Manikandan E, Thanigai AK, Magesh S, Kalyanaraman R, Maaza M. 2016. Green synthesis of silver nanoparticles using *Piper nigrum* concoction and its anticancer activity against MCF-7 and Hep-2 cell lines. J Antimicrob Agents 2: (3): 1-5. DOI: 10.4172/2472-1212.1000123.

Lagashetty A, Ganiger SK, Shashidhar. 2019. Synthesis, characterization and antibacterial study of Ag-Au Bi-metallic nanocomposite by bioreduction using *Piper betle* leaf extract. Heliyon 5: e02794. DOI: 10.1016/j.heliyon.2019.e02794.

Larsson DG, Flach CF. 2022. Antibiotic resistance in the environment. Nat Rev Microbiol 20: 257-269. DOI: 10.1038/s41579-021-00649-x.

Lazar V, Holban AM, Curutiu C, Chifiriuc MS. 2021. Modulation of quorum sensing and biofilms in less investigated Gram-negative ESKAPE pathogens. Front Microbiol 12: 676510. DOI: 10.3389/fmicb.2021.676510.

Mahiuddin M, Saha P, Ochiai B. 2020. Green synthesis and catalytic activity of silver nanoparticles based on *Piper chaba* stem extracts. Nanomaterials 10: 1777. DOI: 10.3390/nano10091777.

Masum MMI, Siddiqa MM, Ali KA, Zhang Y, Abdallah Y, Ibrahim E, Qiu W, Yan C, Li B. 2019. Biogenic synthesis of silver nanoparticles using *Phyllanthus emblica* fruit extract and its inhibitory action against the pathogen *Acidovorax oryzae* strain RS-2 of rice bacterial brown stripe. Front Microbiol 10: 820. DOI: 10.3389/fmicb.2019.00820.

Murray CJ, Ikuta KS, Sharara F, Swetschinski L, Aguilar GR, Gray A, Naghavi M. 2022. Global burden of bacterial antimicrobial resistance in 2019: A systematic analysis. The Lancet 399: 629-655. DOI: 10.1016/S0140-6736(21)02724-0.

Ozdal M, Gurkok S. 2022. Recent advances in nanoparticles as antibacterial agent. ADMET DMPK 10: 115-129. DOI: 10.5599/admet.1172.

Paulkumar K, Gnanajobitha G, Vanaja M, Rajeshkumar S, Malarkodi C, Pandian K, Annadurai G. 2014. *Piper nigrum* leaf and stem assisted green synthesis of silver nanoparticles and evaluation of its antibacterial activity against agricultural plant pathogens. Sci World J 2014: 829894. DOI: 10.1155/2014/829894.

Rosyidah A, Nantapong N, Chudapongse N, Weeranantanapan O, Limphirat W. 2021. Optimization of silver nanoparticles synthesis by the green method using *Streptomyces sp*. SSUT88A and their antimicrobial activity against *Pseudomonas aeruginosa*. IOP Conf Ser Earth Environ Sci 948: 012085. DOI: 10.1088/1755-1315/948/1/012085.

Santhoshkumar R, Hima Parvathy A, Soniya EV. 2021. Phytosynthesis of silver nanoparticles from aqueous leaf extracts of *Piper colubrinum*:

Characterisation and catalytic activity. J Exp Nanosci 16: 294-308. DOI: 10.1080/17458080.2021.1970140.

Theos KR, Johnson KM, Johnson DW. 2019. *Staphylococcus aureus* antibiotic susceptibilities in infections in an outpatient dermatology office on O 'ahu. Hawai'I J Med Public Health 78 (5): 163-168.

Vijayakumar M, Priyab K, Nancyb FT, Noorlidaha A, Ahmed ABA. 2013. Biosynthesis characterization and anti-bacterial effect of plant-mediated silver nanoparticles using *Artemisia nilagirica*. Ind Crops Prod 41: 235-240. DOI: 10.1016/j.indcrop.2012.04.017.

Weeranantanapan O, Chudapongse N, Limphirat W, Nantapong N. 2022. *Streptomyces chiangmaiensis* SSUT88A mediated green synthesis of silver nanoparticles: Characterization and evaluation of antibacterial action against clinical drug-resistant strains. RSC Adv 12: 4336-4345. DOI: 10.1039/d1ra08238h.